Vaccine 42 (2024) 3474–3485

Contents lists available at ScienceDirect

Vaccine

journal homepage: www.elsevier.com/locate/vaccine

VLPs generated by the fusion of RSV-F or hMPV-F glycoprotein to HIV-Gag show improved immunogenicity and neutralizing response in mice

Benjamin Trinité [a,*], Eberhard Durr [b], Anna Pons-Grífols [a], Gregory O'Donnell [b], Carmen Aguilar-Gurrieri [a], Silveria Rodriguez [b], Victor Urrea [a], Ferran Tarrés [a], Joel Mane [b], Raquel Ortiz [a], Carla Rovirosa [a], Jorge Carrillo [a], Bonaventura Clotet [a,c], Lan Zhang [b,*], Julià Blanco [a,c,d,e,*]

[a] IrsiCaixa, Badalona, Spain
[b] Merck & Co., Inc., Rahway, NJ, USA
[c] University of Vic-Central University of Catalonia (UVic-UCC), Vic, Spain
[d] Germans Trias i Pujol Research Institute (IGTP), Badalona, Spain
[e] CIBERINFEC, Madrid, Spain

ARTICLE INFO

Keywords:
Respiratory syncytial virus
Human metapneumovirus
Vaccine
HIV Gag
Fusion protein
Virus like particles
Immunogenicity
Neutralizing antibodies

ABSTRACT

SUMMARY: Respiratory syncytial virus (RSV) and human metapneumovirus (hMPV) vaccines have been long overdue. Structure-based vaccine design created a new momentum in the last decade, and the first RSV vaccines have finally been approved in older adults and pregnant individuals. These vaccines are based on recombinant stabilized pre-fusion F glycoproteins administered as soluble proteins. Multimeric antigenic display could markedly improve immunogenicity and should be evaluated in the next generations of vaccines. Here we tested a new virus like particles-based vaccine platform which utilizes the direct fusion of an immunogen of interest to the structural human immunodeficient virus (HIV) protein Gag to increase its surface density and immunogenicity. We compared, in mice, the immunogenicity of RSV-F or hMPV-F based immunogens delivered either as soluble proteins or displayed on the surface of our VLPs. VLP associated F-proteins showed better immunogenicity and induced superior neutralizing responses. Moreover, when combining both VLP associated and soluble immunogens in a heterologous regimen, VLP-associated immunogens provided added benefits when administered as the prime immunization.

1. Introduction

Respiratory syncytial virus (RSV) and human metapneumovirus (hMPV) are closely related human orthopneumoviruses and major etiological agents of acute respiratory infections in humans [1]. Severe disease mostly affects young children, individuals with chronic respiratory or heart conditions, and older adults. In the latter group, mortality is comparable to the one of influenza A [2]. In children, while infection associated deaths primarily occur in developing countries, hospitalizations remain an economic burden in developed countries [3].

Vaccines for both RSV and hMPV are long overdue, but their development had been delayed following initial setbacks in the 1960's when a formalin-inactivated RSV vaccine tested in children led to enhanced disease and the death of two toddlers. After long and careful studies of RSV immunology, the development of RSV vaccines took a new momentum in the last decade with the elucidation of the RSV Fusion glycoprotein (RSV-F) post-fusion and pre-fusion atomic structures [4–6]. Neutralizing antibodies, following infection or passive immunization, have been associated with disease protection [7–11], however, neutralizing epitopes are mostly exposed on a metastable pre-fusion RSV-F and vaccine clinical trials using post-fusion F protein were unsuccessful in eliciting sufficient neutralizing responses. Advances in structure-based vaccine design permitted the creation of the first stabilized pre-fusion recombinant RSV-F, DS-CAV-1, via the introduction of a disulfide (DS) bond between S155C and S290C mutations and cavity-filling (CAV) mutations S190F and V207L [12]. This paved the way for the development of new recombinant RSV vaccine candidates. Several vaccine candidates are now in late clinical trial stage showing

* Corresponding authors at: IrsiCaixa AIDS Research Institute, Can Ruti Campus, UAB, Badalona, Spain (J.B.).
E-mail addresses: btrinite@irsicaixa.es (B. Trinité), lan_zhang2@merck.com (L. Zhang), jblanco@irsicaixa.es (J. Blanco).

https://doi.org/10.1016/j.vaccine.2024.04.048
Received 9 January 2024; Received in revised form 26 March 2024; Accepted 14 April 2024
Available online 18 April 2024

promising results. Two pre-fusion F glycoprotein-based vaccines, from GlaxoSmithKline Biologicals (AREXVY) and Pfizer (ABRYSVO), have been recently approved for the first time for older adults, and the latter vaccine was also approved for pregnant individuals.

High density of immunogens on particles can induce stronger immune responses when compared with soluble recombinant proteins [13–15]. Therefore, Virus-like particles (VLPs), which derive from the expression of one or more viral structural proteins, represent a promising platform for the display of multimeric antigens. Efficacy of VLP-based vaccines has already been demonstrated for both RSV and hMPV in animal models [16–21] and recently, a highly engineered VLP-based bivalent RSV [22] and hMPV vaccine, IVX-A12 (Icosavax) has reached phase 2 clinical trial. VLPs can derive from enveloped or non-enveloped viruses ([23] for review). Non-enveloped VLPs are a well-organized assembly of structural proteins and can display immunogens with a geometrically controlled density. Enveloped VLPs possess a lipidic membrane, they can accommodate more complex surface proteins and provide a native-like platform for vaccines targeting enveloped viruses such as human immunodeficiency virus (HIV-1) or RSV/hMPV. HIV derived VLPs can easily be produced by expression of a single structural protein, Gag. However, the incorporation of immunogens at their surface is not optimal. We recently developed a new approach to increase the density of displayed immunogens at the surface of the VLPs [24]. This strategy consists in the expression of a unique fusion protein combining HIV-1 Gag with an immunogen of interest. We already tested this concept with HIV-1 [24] and feline leukemia virus (FeLV) [25] derived immunogens, obtaining VLPs with a higher density of surface immunogens.

Here, we applied our Gag fusion strategy for the creation of both RSV- and hMPV-F vaccines. We designed RSV-F-Gag and hMPV-F-Gag fusion constructs, validated the corresponding VLP production and antigenicity *in vitro* and optimized their purification. We then performed immunizations in mice comparing VLP-associated and soluble F proteins. VLP-associated F proteins demonstrated better immunogenicity after prime immunization and better neutralizing response following booster immunization.

2. Results

2.1. RSV-F vaccine strategy

Our working hypothesis was that displaying high density of RSV-F immunogen at the surface of VLPs would generate a better humoral response than the soluble form of the equivalent RSV-F immunogen. In order to generate such VLPs, we utilized a previously described RSV-F pre-fusion stabilized immunogen, sc9-10 DS-Cav1 A149C Y458C S46G N67I E92D S215P K465Q (referred here as VRC4) [26] which we fused to the HIV-1 structural protein Gag. VRC4 is a structure-based engineered immunogen designed as an improved version of DS-CAV-1 [12]. In addition to DS-CAV-1 modifications, it included: a GS linker between residues 105 and 145 (Fig. 1A), in place of pep27 and the fusion peptide, directly connecting the F_1 and F_2 domains; an additional disulfide bond enabled by A149C and Y458C mutations; and additional mutations, S46G, N67I, E92D, S215P, L373R and K465Q, for increased pre-fusion stability and/or expression. We restored the RSV-F transmembrane domain to VRC4 (mVRC4) and fused mVRC4 to HIV-1 Gag via a flexible GS linker (Fig. 1A). To define the final design, we first analyzed the potential impact of the Cysteine 550 located in the cytoplasmic domain of F protein close to the RSV-F and HIV Gag junction. This residue is known to be palmitoylated [27] but not required for protein expression or function [28]. Since palmitoylation could impact membrane localization and hence influence VLP formation, we constructed two mVRC4-Gag fusion proteins containing or lacking C550. No differences were observed in protein expression or VLP formation between each construct (data not shown) and we decided to exclude this residue from the final protein design. Gag was fused via a flexible GS linker directly after the transmembrane domain, in C-terminal of L548. Importantly, the association of HIV-1 Gag with a transmembrane domain redirects Gag oligomerization along the intracellular secretory pathway which leads to intracellular VLP budding [25].

2.2. mVRC4-Gag and VLP_{VRC4} antigenicity

In a first round of experiments, we evaluated the antigenicity of mVRC4-Gag fusion proteins, expressed in Expi293F cells (Fig. 1B), against a panel of human (or humanized) and mouse anti-RSV-F antibodies [29–33] specific for previously described characteristic epitopes [5,29] present in pre- and/or post-fusion RSV-F ([34] for review). As expected, signal was increased in permeabilized cells because of intracellular VLP budding and protein accumulation. All the main neutralizing epitopes were recognized, including sites Φ and V as well as a trimeric F-specific epitope which are all characteristic of pre-fusion RSV-F. These data along with the absence of recognition by the post-fusion specific antibody 4D7 also indicated that RSV-F proteins were properly stabilized in a trimeric prefusion conformation, as expected. Intracellular budding could be confirmed by transmission electronic microscopy (TEM) on transfected cells (Fig. 1C) showing VLPs formed with a size of roughly 100 to 150 nm in diameter. In order to recover these VLPs, we performed a detergent extraction step adapted from the work of the Titchener-Hooker group [35,36] and which we described previously [25]. After extraction, VLPs (VLP_{VRC4}) could be identified by cryogenic-TEM (cryo-EM) together with cell debris (Fig. 1D). Maintenance of pre-fusion RSV F antigenic sites for these extracted VLPs was assessed by ELISA using the previously mentioned RSV-F antibody panel as capture antibodies and an HRP-conjugated polyclonal anti-Gag antibody for detection (Fig. 1E). The antigenic profile was reminiscent of cellular staining confirming the presence of all key neutralizing epitopes as well as the presence of trimeric RSV-F.

2.3. VLP_{VRC4} purification and quantification

To better isolate extracted VLPs from cell debris and other soluble proteins, we established a purification strategy (Fig. S1A), which included ultracentrifugation on a double sucrose cushion (30 %/70 %), dialysis using a 100 kDa MWCO membrane to remove the excess of sucrose, and filtration at 0.45 μm for sterilization. All steps were performed in sterile conditions to minimize possible contamination and subsequent endotoxin accumulation. After ultracentrifugation (Fig. S1B), each fraction was collected and analyzed on SDS-page gels. While total proteins were visualized by Coomassie stain (Fig. S1C), mVRC4-Gag protein was identified by western blot using an anti-Gag polyclonal antibody (pAb) (Fig. S1D). Most contaminating proteins were retained before the 30 % sucrose cushion and Gag signal was enriched at the interphase of the 30 % and 70 % sucrose (fraction 4), immediately below (fraction 5) and also present in the 70 % cushion (Fraction 6). We retained fractions 4 and 5 for vaccine production. These fractions were mixed and dialyzed using a 100 kDa MWCO membrane in sterile PBS and filtered at 0.45 μm for sterilization. The final production was quantified by western blot comparing the VLP associated RSV-F protein and a standard of soluble recombinant VRC4 RSV-F, the same protein used subsequently as protein control for animal immunization (Fig. S1E). After final filtration, purified mVRC4-Gag VLP (VLP_{VRC4}) were obtained at a concentration of 2.4 μg/mL of soluble VRC4 protein (Pro_{VRC4}) equivalent (Table 1). We also verified the endotoxin content which was well below the required maximum level of 0.15 endotoxin unit (EU) per injection for in vivo immunization [37] (Table 1).

Finally, we performed a mass spectrometry (MS) analysis to characterize the protein content of our VLP_{VRC4} vaccine preparation. MS sequence coverage of the mVRC4-Gag fusion protein was 46.4 % (Fig. S1F and Table 1) and mVRC4-Gag peptides contributed 1.9 % of the MS signal of all identified peptides (Table 1). All other proteins detected were of human origin (from producer cells), notably including heat

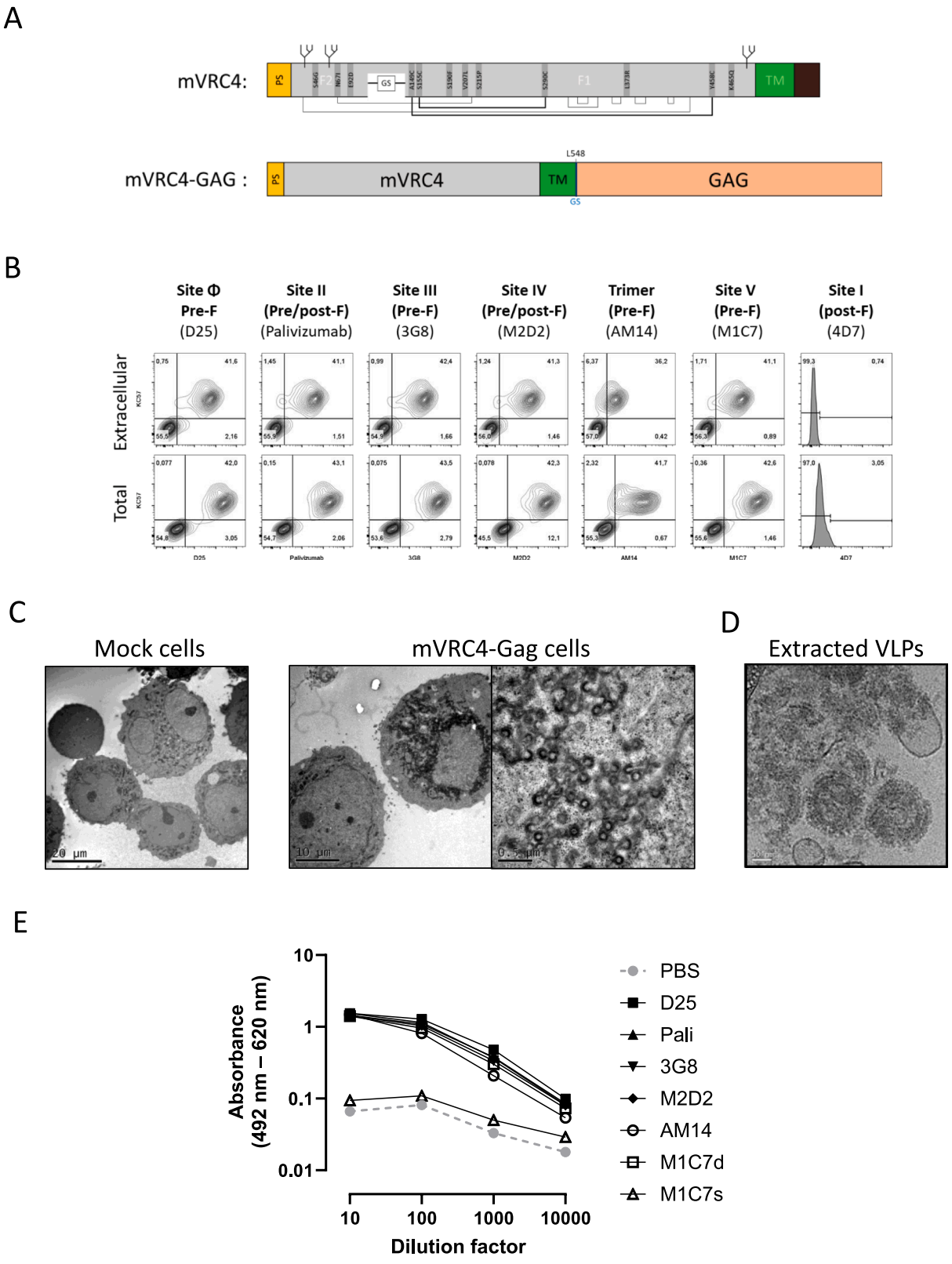

Fig. 1. Antigenicity of VRC4-Gag based VLPs. A. Schematic representing mVRC4 and mVRC4-Gag constructs. PS = peptide signal, TM = transmembrane domain. For mVRC4, glycosylation sites are indicated on top, and disulfide bounds at the bottom (thin lines indicate natural RSV-F disulfide bounds while thick lines indicate artificial bounds consecutive to amino acids substitutions). For mVRC4-Gag construct the truncation position (residue 548) is indicated on top. B. Surface and total antigenicity of mVRC4-Gag measured by flow cytometry in transfected Expi293F cells. C. TEM on mVRC4-Gag and mock transfected Expi293F cells highlighting intracellular VLP accumulation. D. Cryo-EM on extracted mVRC4-Gag VLPs. E. Sandwich ELISA on extracted mVRC4-Gag VLPs using the indicated capture antibodies and an HRP-conjugated anti-HIV-1 p17p24p55 Gag pAb for detection.

Table 1
VLP_{VRC4} and VLP_{hMPV-F} post-purification analyses.

	VLP_{VRC4}	VLP_{hMPV-F}
Quantification:		
RSV-F or hMPV-F concentration (ug/mL)	2.4	9.83
Endotoxin:		
Endotoxin concentration (EU/mL)	0.21	0.18
Endotoxin per injection of 100 ng RSV-F (EU)	0.009	0.002
Mass-Spec analysis:		
Coverage [%]	46	67
# Peptides	26	48
% MS signal	1.95	8.49

shock protein 70, ribonucleoproteins and ribosomal proteins (Fig. S1G).

2.4. VRC4 immunization in BALB/c mice

To first evaluate the immunogenicity of VLP_{VRC4}, we immunized BALB/c female mice with 2 doses of a homologous vaccine regimen including either 100 ng of Pro_{VRC4} protein formulated with Merck amorphous aluminum hydroxylphosphate sulfate (MAA, Merck & Co., Inc., Rahway, NJ, USA), 100 ng RSV-F equivalent of VLP_{VRC4} formulated with or without MAA, or MAA alone (Fig. 2A). Second immunization was performed 4 weeks apart and sera were collected 2 weeks after each immunization (PD1 and PD2). The level of antibody against pre-fusion (Fig. 2B) and post-fusion (Fig. S2) RSV-F was determined by ELISA. Soluble recombinant pre-fusion, but not post-fusion RSV-F used as the coating antigen in the ELISA assays, contains a foldon domain in the C-terminal which can account for some of antibody binding reactivity observed in the sera of animals immunized with soluble protein-based (which also contains the foldon domain), but not VLP-based vaccines. Therefore, we measured antibodies against both pre- and post-fusion RSV-F to control for non-relevant anti-foldon responses. At PD1, animals immunized with Pro_{VRC4} + MAA had low or undetectable levels of RSV-F specific antibodies (GM = 51) probably because of the low dose of immunogen (Fig. 2B). Similarly, in the absence of adjuvant, only a few mice immunized with VLP_{VRC4} showed RSV-F specific antibodies (GM = 45). In sharp contrast, when VLP_{VRC4} were formulated with MAA, RSV-F antibodies were detected in all animals and the PD1 antibody level (GM = 1199) was statistically superior to Pro_{VRC4} + MAA ($p = 0.0014$) and VLP_{VRC4} alone ($p = 0.0014$). Results were similar when measuring anti-post-fusion F specific response (Fig. S2A). At PD2, all anti-pre-fusion RSV-F responses were clearly boosted by the second immunization (Fig. 2C). Notably, while Pro_{VRC4} + MAA induced response was low at PD1, at PD2 it was superior to VLP_{VRC4} without adjuvant ($p = 0.00196$) and equivalent to the response from VLP_{VRC4} + MAA (p = ns). In terms of

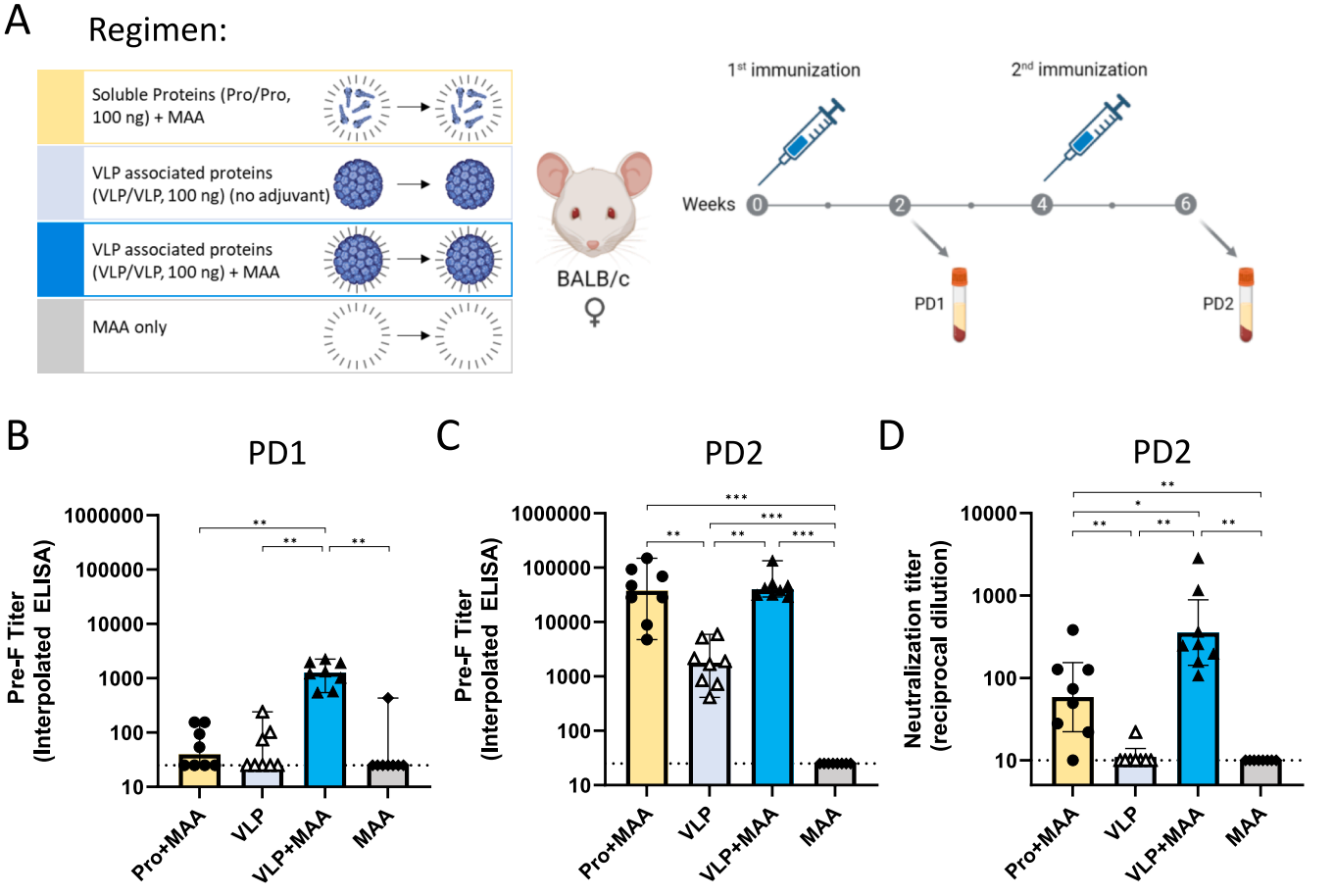

Fig. 2. Immunogenicity of mVRC4-Gag based VLPs in BALB/c mice. A. Schematic representing the immunization regimen and timeline of immunizations and blood collection. B/C. ELISA quantification of (B) anti-pre-fusion humoral responses at PD1 (B) and PD2 (C) in heat inactivated serum collected 2 weeks after each immunization. Bars indicate geometric means. As many sera yielded undetected results, comparisons were performed with a Peto-Peto test. Significant p values are indicated and were corrected for multiple comparison (**p < 0.01, ***p < 0.001). Dashed lines indicate the assay lower limit of detection (=25). D. Anti-RSV-F neutralization titers in sera collected 2 weeks after second immunization. Titers are expressed in reciprocal dilution. Bars indicate geometric means. As many sera yielded undetected results, comparisons were performed with a Peto-Peto test. Significant p values are indicated and were corrected for multiple comparison (*p < 0.05, **p < 0.01). Dashed lines indicate the assay lower limit of detection (=10).

immunogenicity, VLP_{VRC4} + MAA, which was superior to Pro_{VRC4} + MAA at PD1, lost its advantage at PD2, suggesting that this specific VLP regimen was not optimal for boosting.

PD2 sera were then tested for their neutralizing activity against RSV. Only immunization regimens that included MAA adjuvant (Pro_{VRC4} + MAA and VLP_{VRC4} + MAA) were able to induce a significant neutralizing response. Notably, while VLP_{VRC4} alone did not elicit any detectable neutralizing responses, VLP_{VRC4} + MAA generated a greater neutralizing response than Pro_{VRC4} + MAA (Geo Mean: 355 vs 58, $p = 0.014$, Fig. 2D), even though the two vaccines induced comparable binding antibody titers.

Altogether, this data indicates that VRC4 immunization as a VLP-displayed immunogen was more effective at primary immunization and generated a better neutralizing response than soluble VRC4. However, the boost conferred by the second immunization was probably not optimal with the tested VLP regimen. This could be explained by the presence of human host proteins in the VLP-based vaccine, which might interfere with a VRC4 focused response during the second immunization. Therefore, we hypothesized that a heterologous regimen combining VLP-displayed immunogen and soluble VRC4 protein could avoid repeated anti-human protein stimulation and provide a better boost.

2.5. hMPV-F VLP vaccine

Before proceeding with a second immunization experiment, we decided to generate an additional vaccine candidate targeting hMPV-F. In this case, hMPV-F-Gag was based on the wild-type (WT) unmodified extracellular and transmembrane domains sequence of hMPV-F and was fused to HIV-1 Gag after the transmembrane domain, C-terminal of K516 (Fig. 3A). Antigenicity was first verified in transiently transfected Expi293F cells. Among our panel of F specific antibodies, all four antibodies with known reactivity against hMPV-F (3G8, M2D2, M1C7 and M1C7s) showed strong recognition demonstrating good presentation of antigenic sites II, III, IV, and most importantly V (Fig. 3B). As with mVRC4-Gag, intracellular signal was superior, therefore, predicting intracellular accumulation of VLPs. TEM on transfected cells confirmed the presence of VLP like elements in the cellular secretory pathway (Fig. 3C). Following extraction, we confirmed by cryo-EM the presence of VLPs with a diameter of about 100 nm (Fig. 3D). Antigenicity of extracted VLPs was analyzed by ELISA showing a very similar profile to the one observed by flow cytometry (Fig. 3E). Extracted VLPs were subsequently purified following the same strategy described for VLP_{VRC4}. Following sucrose gradient ultracentrifugation, we retained fractions 4, 5 and 6 (Fig. S3A–C). After dialysis and final filtration, VLP_{hMPV-F} preparation was quantified by western blot against recombinant hMPV-F protein. Notably, final concentration of VLP_{hMPV-F} was increased in comparison to VLP_{VRC4} (Fig. S3D and Table 1). Endotoxin level was minimal.

Final MS analysis indicated a better overall purity (8.49 % MS signal, Table 1) and coverage (Fig. S2E) of VLP_{hMPV-F} in line with the increased concentration as compared to VLP_{VRC4}. Host protein contaminants were of similar origin as in the VLP_{VRC4} preparation (Fig. S3F–G).

2.6. Homologous and heterologous VRC4 and hMPV-F immunization in C57Bl/6JOlaHsd mice

For this second immunization experiment, we used male and female C57Bl/6JOlaHsd mice, and we compared homologous and heterologous immunization regimes combining 100 ng of VLP-associated and/or soluble immunogen (Fig. 4A), for either RSV or hMPV-F. All immunizations were formulated with aluminum phosphate adjuvant (InvivoGen, AdjP). For heterologous prime/boost immunizations, VLP based vaccines were administered either as first or second dose. In the specific case of VLP_{hMPV-F}, as concentration and purity in the final preparation were higher, we also tested an additional condition with an increased quantity of hMPV-F equivalent VLPs (300 ng) which was injected as first dose followed by a 100-ng dose of soluble hMPV-F.

As already observed in the previous immunization experiment, anti-F antibody responses at PD1 were clearly superior when using the VLP platform compared to soluble protein immunogens. This was true for both, mVRC4 (Fig. 4B, $p = 0.0058$) and hMPV-F (Fig. 4C, 100 *ng* – $p = 0.0003$, *300 ng* – $p = 0.0006$) immunizations. In the case of hMPV-F, immunization with an increased dose of VLP trended to higher antibody response but significance was not reached between 100 and 300 ng doses.

At PD2, as anticipated, the VLP/Pro strategy was the better option for VRC4 immunization (Fig. 4D) as compared to the Pro/Pro strategy ($p = 0.03$), confirming that VLPs serve as a better priming vaccine. Interestingly, heterologous VLP/Pro regimen was also superior to the VLP/VLP homologous regimen ($p = 0.046$), corroborating our hypothesis that immune responses after homologous VLP_{VRC4} vaccination may have been suppressed due to the presence of human host-cell proteins. In the case of hMPV-F, VLP/VLP immunization seemed more in line with other combinations and no statistical difference was observed, possibly because the purity of these VLPs was better, which could limit the interference from anti-human protein responses in immunized mice. To assess the anti-human response, we stained Expi293F cells with immunized mouse serums (Fig. S4). PD2 sera of mice who received VLP_{VRC4} or VLP_{hMPV-F} immunization developed antibodies against Expi293F cells and titers were increased when mice received two VLP immunizations (Fig. S4A). Moreover, after PD1, the anti-Expi293F response in mice which received VLP_{hMPV-F} was significantly reduced compared to mice who received VLP_{VRC4} (Fig. S4B), confirming the higher purity of the VLP_{hMPV-F} preparation.

Finally, we measured the neutralizing response after VRC4 and hMPV-F immunizations. While, in the previous immunization experiment, 2 doses of Pro_{VRC4} were sufficient to induce detectable neutralization titers in almost all BALB/c mice (Fig. 2D), only two out of eight immunized C57Bl/6JOlaHsd derived mice show neutralization responses (Fig. 4F), suggesting that the C57Bl/6JOlaHsd mouse model is more restrictive to the generation of anti-F neutralizing antibodies. In this context, both VLP_{VRC4}/Pro_{VRC4} ($p = 0.0054$, neutralization detected in 7 animal out of 8) and VLP_{VRC4}/VLP_{VRC4} ($p = 0.041$; neutralization detected in 4 animal out of 8) immunizations induced significant neutralizing responses. No neutralization was detected with Pro_{VCR4}/VLP_{VRC4} (Fig. 4F). Importantly the heterologous regimen VLP_{VRC4}/Pro_{VRC4} was superior to all other tested groups. Similar results were obtained for the hMPV-F immunization, although in that case only the 300 ng VLP_{hMPV-F}/Pro_{hMPV-F} heterologous regiment induced a significant neutralizing response (Fig. 4G, $p = 0.039$). All together, these data suggest that F antigen displayed on a VLP could induce a better primary response in naïve animals and better neutralizing responses following boosting.

3. Discussion

In this work we generated HIV Gag derived VLP exposing an RSV- or hMPV-F immunogen, directly fused to Gag, as a strategy to increase surface antigen density and induce better B-cell activation. Pre-fusion RSV-F conformation provides the best presentation of neutralizing epitopes [4,6]. Therefore, we built upon a previously described pre-fusion F design [26], referred here as VRC4. mVRC4-Gag antigenicity measured both in producing cells and in particles indicated good presentation of site Φ and V previously described as the most sensitive to neutralization antibodies [12]. In the case of hMPV-F, we tested the possibility to use a wild-type protein sequence which did not include any stabilizing mutation. While soluble forms of F proteins rapidly adopt a post-fusion conformational state [5], membrane bound F protein are more likely to maintain a pre-fusion conformation. In our case, hMPV-F-Gag showed a good exposure of site V both in cells and in particles suggesting a prevalent pre-fusion state. However, the neutralization activity

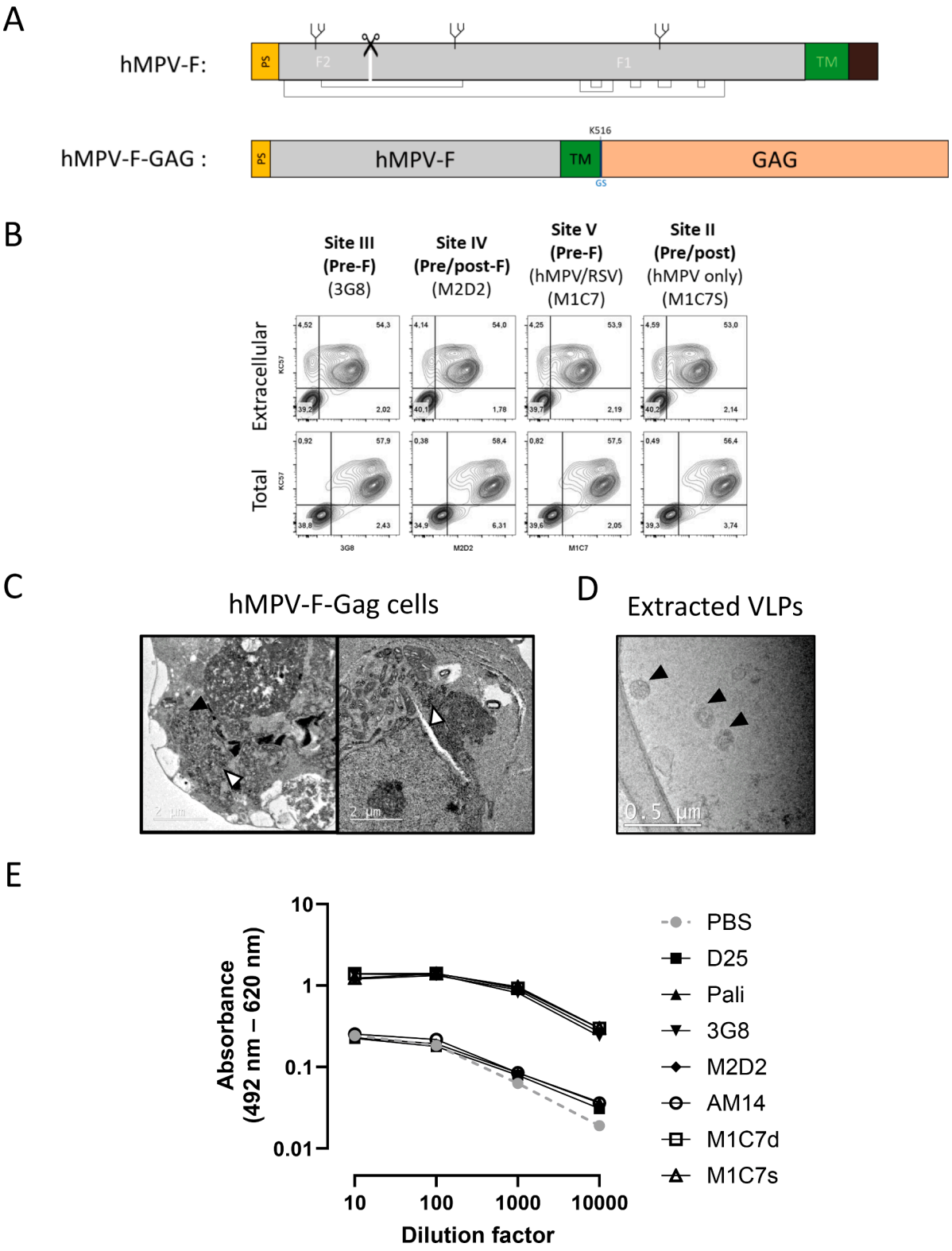

Fig. 3. Antigenicity of hMPV-F-Gag based VLPs. A. Schematic representing WT hMPV-F and hMPV-F-Gag constructs. PS = peptide signal, TM = transmembrane domain. For hMPV-F, glycosylation sites are indicated on top, and disulfide bounds at the bottom. For hMPV-F-Gag construct the truncation position (residue 516) is indicated on top. B. Surface and total antigenicity of hMPV-F-Gag measured by flow cytometry in transfected Expi293F cells. C. TEM on hMPV-F transfected Expi293F cells highlighting intracellular VLP accumulation. D. Cryo-EM on extracted hMPV-F-Gag VLPs. E. Sandwich ELISA on extracted hMPV-F-Gag VLPs using the indicated capture antibodies and an HRP-conjugated anti-HIV-1 p17p24p55 Gag pAb for detection.

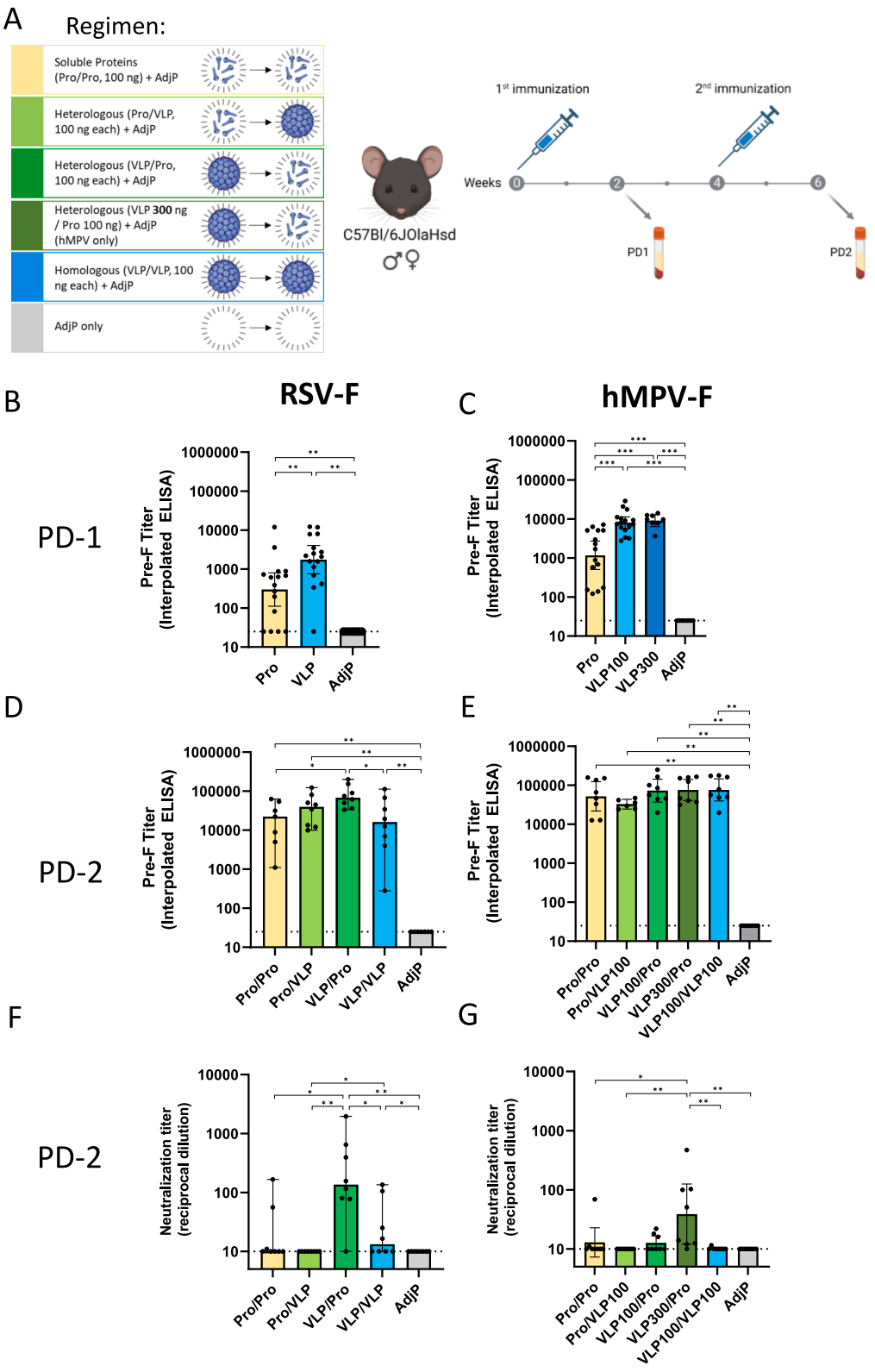

Fig. 4. Immunogenicity of mVRC4-Gag and hMPV-F-Gag based VLPs in C57Bl/6JOlaHsd mice. A. Schematic representing the immunization regimen and timeline of immunizations and blood collection. B/C/D/E. ELISA quantification of anti-pre-fusion RSV-F (B/D) and hMPV-F (C/E) humoral responses in heat inactivated serum collected 2 weeks after first (PD1) and second (PD2) immunizations. Bars indicate geometric means. As many sera yielded undetected results, comparisons were performed with a Peto-Peto test. Significant p values are indicated and were corrected for multiple comparison (*$p < 0.05$, **$p < 0.01$, ***$p < 0.001$). Dashed lines indicate the assay lower limit of detection (=25). F/G. Anti-RSV (F) and hMPV (G) neutralization titers in sera collected 2 weeks after second immunization. Titers are expressed in reciprocal dilution. As many sera yielded undetected results, comparisons were performed with a Peto-Peto test. Significant p values are indicated and were corrected for multiple comparison (*$p < 0.05$, **$p < 0.01$). Dashed lines indicate the assay lower limit of detection (=10).

measured after 2 immunizations was underwhelming and, while increasing the dose of the vaccine to 300 ng of F-protein substantially improved the response, it will be interesting to compare these results with a pre-fusion stabilized hMPV-F immunogen.

We initially hypothesized that immunization with VLPs could preclude the need for adjuvantation, specifically when compared to unadjuvanted soluble proteins, since we had already observed good immune responses in a previous study [24] using an HIV-1 based immunogen in absence of any adjuvant. However, in this study, following first immunization, we only observed a significant response when adjuvant was present. It is important to point out that in this work, animals were immunized with very low doses of vaccines: 100 ng F protein equivalent per injection of RSV-F based vaccine and up to 300 ng F protein equivalent in the case of hMPV. Other works using VLP [16,17,19,38,39] or nanoparticles [22] for RSV-F and or hMPV-F immunization commonly use between 4 ug and 20 ug of F-protein equivalent. In addition, our VLP preparations had very low endotoxin content, less than 0.02 EU per injection, which is well below the recommended limit of 0.15 EU per injection [37]. In this context, and in the presence of aluminum adjuvant (MAA or AdjP), a first injection with VLP associated F proteins induced greater response than the equivalent soluble protein. This was true for both RSV and hMPV-F immunizations, suggesting that F-Gag based VLPs provide better immunogenicity in comparison to soluble proteins in naïve animals. Importantly, our VLP preparations were directly quantified against the respective recombinant soluble F protein that were used for mouse immunization, ensuring the fairest comparison.

After the second homologous immunization, the benefits of our VLP platform faded in terms of total anti-F specific humoral response, suggesting that the VLP associated F immunogens failed to properly boost the response in comparison to the protein–protein regimen. We hypothesized that this was due to the presence of human host proteins as part of the VLPs preparation which could induce anti-human protein response after primary immunization and this response could interfere with boosting using VLPs containing the same impurity. Interestingly though, despite the protein–protein regimen showing similar end-point antibody binding titers, the neutralizing response obtained after two consecutive VLP displayed F protein immunization was still statistically superior to the protein–protein immunization. This suggests that VLP based immunization provided a qualitative benefit which translated in higher neutralizing potency. To better optimize the F immunogen for the second immunization, we tested a heterologous regimen VLP/Pro. As anticipated, VLP/Pro led to higher binding and neutralizing antibody responses which were statistically superior to the Pro/Pro regimen. Differences between regimen were less pronounced with the hMPV-F vaccine although trends were similar. Interestingly, the opposite regimen, Pro/VLP, failed to induce a comparable neutralizing activity, suggesting that a specific immunological imprinting was established after the first immunization with soluble protein. Overall, these results show that F-Gag based VLPs provide better immunogenicity in comparison to soluble proteins and most importantly, generate a better neutralizing response. It will be interesting to test the capacity of this platform to induce T-cell responses and ultimately to evaluate the protection against virus challenge in animal model.

Limits of our study include the purity of the VLPs, in term of the presence of human host protein. This could be improved by using more advanced chromatography approaches. hMPV-F-Gag based VLPs reached a higher level of purity (increased "relative MS-signal intensity") probably thanks to a better expression level in producing cells. However, hMPV-F immunizations achieved lower apparent neutralizing responses despite robust binding antibody responses overall. This could be due to the mouse model used (C57Bl/6JOlaHsd mice) and/or the fact that the hMPV-F immunogens did not include stabilizing mutations. Alternative approaches to avoid the need of complex purification processes to remove host proteins, could include the use of nucleic acid-based vaccines encoding for GAG/antigen fusion proteins, producing VLPs in vivo to generate functional humoral responses [24]. Another limit of our work resides in the fact that immunization experiments were performed using two different mouse models in two different locations. BALB/c and C57BL/6 mice are regarded as Th2 and Th1 dominant strains, respectively [40,41], which could influence their capacity to generate neutralizing antibody. There were also meaningful changes in immunization protocols, notably the use, for logistical reason, of similar but not identical adjuvants, and differences in the immunization technics (intramuscular vs hock injection) specific to each center's expertise. Importantly, sera were analyzed by the same team and using the same ELISA and neutralization assays. In this context, both RSV-F immunization studies, performed in different centers, consistently showed the superior immunogenicity and higher neutralizing response of the VLP based vaccines. Finally, while using low dose of immunogens was a guiding principle of this and our previous studies [24], improving the quantity and purity of the VLP production will be critical to evaluate the precise amount of immunogen required and take fully advantage of our Gag fusion protein based VLP platform.

4. Methods

4.1. Antibodies

For the characterization of RSV-F and hMPV-F antigenicity, we used the human antibodies D25 [30], AM14 [30], 3G8 [31], M2D2 [31], M1C7 [31], M1C7s [32], the humanized antibody, Palivizumab [33] and the mouse antibody 4D7 [29].

4.2. Soluble VRC4 and hMPV-F proteins

The plasmid construction and production of RSV PreF (VRC4) was performed as previously described [26]. The hMPV-F trimeric antigen was derived from a previously published F sequence of strain B2 with a C-terminal GCN4 trimerization domain [42]. All constructs have a C-terminal thrombin cleavage site, followed by a 6xHis tag and a strep-tag. Sequences were codon-optimized for mammalian expression (Life Technologies and Genewiz), cloned into an expression vector, and transiently transfected into Expi293 suspension cells (Thermo Fisher Scientific). On days 3 post-transfection, supernatants were harvested for western blot to confirm expression and for large-scale purification. The purification of all antigens was performed as previously described [29,31]. Briefly, harvested supernatants with His-tagged proteins were captured by Ni-Sepharose chromatography (GE Healthcare, USA) and eluted by high imidazole concentration. In course of an overnight dialysis in the presence of thrombin, the His-tag was cleaved, and the concentration of imidazole was reduced. Uncleaved His-tag products, as well as initial Ni-Sepharose non-specific binding impurities, were removed by negative Ni- Sepharose chromatography (product in flow-through). The protein antigens were further purified by size-exclusion chromatography (Superdex 200, GE Healthcare) and stored in a buffer of 50 mM HEPES pH 7.5 with 300 mM NaCl.

4.3. Cell lines

The Expi293F cell line (ThermoFisher Scientific, USA) was used for VLP production. Cells were cultured in Expi293 Expression Medium (Gibco, Thermo Fisher Scientific) at 37 °C, 8 % CO2, and under agitation at 125 rpm.

4.4. Plasmids

All DNA sequences were synthesized at GeneArt (Thermo Fisher Scientific, Waltham, MA, USA) and subcloned into the pcDNA3.4-TOPO vector (Thermo Fisher Scientific, Waltham, MA, USA). All plasmids were transformed into One Shot TOP10 Chemically Competent E. coli (Invitrogen) for plasmid DNA amplification. Plasmids were purified in

endotoxin-free conditions using the ZymoPure II Plasmid Maxiprep Kit (Zymo Research) and sterile filtered at 0.22 μm (Millipore).

4.5. Expression

Expi293F cells were transiently transfected with mVRC4-Gag or hMPV-F-Gag expression plasmids using ExpiFectamine transfection reagents (Gibco) following the manufacturer's instructions. Notably, 20 h after transfection cell medium was supplemented with enhancer reagents (Gibco). Cells were harvested at 48 h after transfection. Supernatant was kept for analysis.

4.6. Flow cytometry analysis of antigenicity

Expi293F cells transfected with mVRC4-Gag or hMPV-F-Gag were stained extracellularly and or intracellularly with a panel of RSF-F and hMPV-F specific human monoclonal antibodies (described above) revealed by an APC-labeled anti-human IgG (Fcγ) (Jackson ImmunoResearch) and intracellularly with a FITC-conjugated HIV-1 p24 Gag specific antibody (mouse, KC57; Beckman Coulter, USA). Extracellular staining was performed in PBS. For intracellular staining, cells were first fixed with fixation buffer (Medium A; Invitrogen/Thermo Fisher Scientific) and stained in permeabilizing conditions with permeabilization buffer (Medium B; Invitrogen/Thermo Fisher Scientific). For the detection of site-I post-fusion epitope, cells were stained with a mouse monoclonal antibody 4D7 (described above). In that specific case, cells were not dual stained with anti-HIV-1 p24 Gag antibody KC57 which is also a mouse antibody, to avoid interference. Stained cells were acquired on a BD FACSCelesta™ Cell Analyzer (BD, USA) with FACSDiva™ Software version 8.0.1.1 (BD) and analyzed with FlowJo™ v10.6.1 Software (BD).

4.7. Transmission electron microscopy (TEM)

Cells producing VLPs were analyzed by transmission electron microscopy (TEM). Briefly, transiently transfected Expi293F cells were fixed with 2.5 % glutaraldehyde in PBS 0.1 M for 2 h at 4 °C, post-fixed with 1 % osmium tetroxide with 0.8 % potassium ferrocyanide for 2 h and dehydrated in increasing concentrations of ethanol. Then, pellets were embedded in epon resin and polymerized at 60 °C for 48 h. Sections of 70 nm in thickness were obtained with a Leica EM UC6 microtome (Wetzlar), stained with 2 % uranyl acetate and Reynold's solution (0.2 % sodium citrate and 0.2 % lead nitrate), and analyzed using a JEM-1400 transmission electron microscope (Jeol Ltd., Akishima, Japan). All images were taken at 120 kV.

4.8. VLP extraction

Recovery of intracellular VLPs was adapted from Titchener-Hooker, N. et al. [35,36]. Cell pellets were resuspended in 1 pellet volume (PV) of ice-cold lysis buffer: PBS pH 7.4 (Gibco), 2 mM EDTA (Thermo Fisher Scientific, Waltham, MA, USA), 2 mM EGTA (Merck, Darmstadt, German), and Protease Inhibitor (Complete™ ULTRA Tablets EDTA-free, Merck, Darmstadt, German). Cells suspensions were homogenized with a tissue grinder (CS1, KIMBLE) for 1 min on ice. 2 PV of lysis buffer supplemented with 0.2 % final Triton X-100 were added and cells were incubated for 4 h at 4 °C under rotation to ensure VLP release. Centrifugation at 3000 × g for 15 min was carried out to remove cellular debris and contaminants. Finally, supernatants were incubated with Amberlite XAD-4 beads (Merck, Darmstadt, German) for 2 h at 4 °C for Triton X-100 removal. VLP containing supernatant were recovered after filtration through a 70 μm mesh (Greiner bio-one, Kremsmünster, Austria) to remove the beads.

4.9. ELISA analysis of antigenicity

In order to characterize mVRC4-Gag and hMPV-F-Gag antigenicity on extracted particles we performed a sandwich ELISA combining a capture step utilizing the panel of RSV-F and hMPV-F specific monoclonal antibodies described above and detection staining with and Anti-HIV-1 p55 + p24 + p17 Gag antibody (Rabbit, ab63917; Abcam, UK) followed by HRP-conjugated AffiniPure F(ab')$_2$ Fragment Donkey Anti-Rabbit IgG (H + L) (Jackson ImmunoResearch, USA). Capture antibodies were coated overnight in PBS at 4 °C in Nunc Maxisorp ELISA plates (Thermo Fisher Scientific). Plates were then blocked with 1 % BSA PBS (without detergent) for 2 h at room temperature. Various dilutions of VLP preparation were incubated in the plate overnight at 4 °C. After washing with PBS 0.05 % Tween 20, plates were incubated for 1 h at room temperature with detection antibody diluted in blocking buffer. After washes, plates were incubated for another hour at room temperature with the HRP-conjugated secondary antibody and finally plates were developed with o-Phenylenediamine dihydrochloride (OPD) (Sigma Aldrich, St. Louis, MO, USA) and stopped using 2 N of H2SO4. The signal was analyzed on an EnSight Multimode Plate Reader (PerkinElmer, USA) at 492 nm with noise correction at 620 nm.

4.10. Cryogenic transmission electron microscopy (cryo-EM)

Extracted VLP preparations were analyzed by cryo-EM. VLPs were deposited on a carbon-coated copper grid and prepared using a Leica EM GP workstation (Leica). VLPs were observed with a Jeol JEM-2011 (Jeol Ltd., Akishima, Japan), equipped with a CCD 895 USC4000 camera (Gatan, Pleasanton, CA, USA).

4.11. VLP purification

Samples were further purified by ultracentrifugation in a 70 %/30 % double sucrose cushion at 28,000 × g for 2.5 h at 4C. After centrifugation, each fraction was recovered separately (Fig. S1B) and analyzed by western blot (see below). Fractions of interest were further treated for sucrose removal by dialysis with 100 kDa MWCO Spectra-Por Float-A-Lyzer G2 (Merck, Darmstadt, German) following the manufacturer's recommendation against 1 × PBS at 4C. The final sucrose concentration in VLP vaccine preparation was expected to be lower than 5 %. Finally, VLP preparation were filtered through 0.45 μm pore size (Millipore).

4.12. Coomassie and western blot characterization

Samples were treated with reducing agent (Thermo Fisher Scientific), boiled for 5 min at 95 °C and subjected to electrophoresis in NuPAGE Bis-Tris 4 % to 12 % (Thermo Fisher Scientific).

For coomassie stain, gel was washed in water, incubated 1 h with Coomassie blue under agitation, de-stained overnight in water and acquired on Chemidoc (Bio Rad).

For western blot, proteins were transferred onto a PVDF membrane (Bio-Rad) using the Trans-Blot Turbo Transfer System (Bio-Rad). Membranes were blocked for 1 h at room temperature with blocking buffer (5 % w/v non-fat skim milk powder in PBS 0.05 % Tween20). Membranes were incubated overnight at 4 °C with the primary polyclonal antibodies: Anti-HIV1 p55 + p24 + p17 antibody (Rabbit, ab63917; Abcam), anti-RSV-F (Guinea pig, in-house generated) and anti-hMPV-F (Rabbit, in-house generated). After washing, incubation with the secondary antibody, HRP-conjugated AffiniPure F(ab')$_2$ Fragment Donkey Anti-Rabbit IgG (H + L) (Jackson ImmunoResearch) or HRP-conjugated AffiniPure Donkey Anti-Guinea Pig IgG (H + L) (Jackson ImmunoResearch) was performed for 1 h at room temperature. Membranes were developed using SuperSignal West Pico PLUS Chemiluminescent Substrate (Thermo Fisher Scientific) or SuperSignal West Femto Maximum Sensitivity Substrate (Thermo Fisher Scientific), depending on the band's signal and according to the manufacturer's

protocol.

4.13. Western blot quantification

For protein quantification the VLP preparations were compared against a standard made of the soluble form of the corresponding antigen (VRC4 or hMPV-F as described above). Standard ranged from 7.8 ng to 125 ng. Western blot pictures were analyzed with Image Lab (Bio Rad) and quantification was obtained using the integrated "quantity tool" function.

4.14. Endotoxin detection

Endotoxin measurements were performed by LeanBio (Barcelona) with a standard limulus amebocyte lysate (LAL) method using a Portable Endotoxin Testing System (PTS) from Charles River Laboratories (USA).

4.15. Proteomic analysis

Samples were prepared for bottom-up analysis using the filter aided sample preparation (FASP) method [43] following manufacturer's instructions (FASP protein digestion kit, Abcam ab270519). In brief, VLP samples were concentrated to a volume of 100 µl using a spin filter with a 30 kDa cut of membrane. The VLPs were then denatured by adding 100 µl of 8 M ultra-pure urea (Thermo Fisher). Disulfide bonds were reduced in the filter for 15 min at 65 °C in an incubator shaker by adding 2 µl of 500 mM tris (2-carboxyethyl) phosphine (TCEP, Pierce, bond breaker). Reduction was followed by alkylation with Iodoacetamide. 3 µl of 375 mM freshly prepared Iodoacetamide was added to the filter and then allowed to react for 30 min at room temperature. The enzymatic digestion was performed after clean-up of the reagents using 1:50 (wt/wt) Trypsin/LysC mixture (Promega V5071) per VLP sample. The digestion reaction is performed overnight in an incubator shaker at 37 °C at 400 rpm.

Peptides of the VLP digests were analyzed by nano-LC tandem mass spectrometry using an Orbitap XL mass spectrometer (Thermo Fisher) equipped with an Ultimate 3000 RS nano-HPLC system (Thermo Fisher). One sixth of the peptide mixture from each digest was first captured onto a C-18 µ-trapping column (300 µm ID x 5 mm, C18 PepMap 100P/N 160454, Thermo Fisher) and then back eluted onto a Pico-chip™ analytical tip column (75 µm ID x 10 cm, 15 µm tip ID; New Objective, Littleton, MA) for MS/MS analysis. Peptides were eluted using a 120 min gradient starting at 2 % acetonitrile, linearly progressing within 90 min to 32 % acetonitrile (0.1 % formic acid, EMD suprapure P/N 11670) at a flow rate of 300 nl/min. The analytical portion of the gradient was followed by a cleanup and reconditioning phase. Tandem mass spectra were acquired using top 5, data dependent analysis with dynamic exclusion enabled for 300 s and a repeat duration of 25 s. Raw files were analyzed using the Proteome Discoverer 2.4 software package (Themo Fisher). Extracted ion chromatograms (XIC) were calculated within PD 2.4 to obtain MS signal intensities for VLP and host cell proteins. The XIC contribution for individual proteins was calculated as percentage of the sum total of the XIC of all identified proteins and served as an approximation of protein abundance within each sample. FASTA proteome databases for human proteins were downloaded from uniprot.org.

4.16. Mouse immunogenicity studies

Mouse experiments were performed at 2 different centers and in 2 different mouse strains.

BALB/c mouse studies were performed by the team at Merck & Co., Inc., Rahway, NJ, USA and approved by the Institutional Animal Care and Use Committee (IACUC, APS#2019-600920-Mar) at Merck & Co., Inc., Rahway, NJ, USA. Groups of 8 female BALB/c mice (Charles River Laboratories, USA) aged 6–8 weeks were immunized intramuscularly twice at a 4-week interval. 100 uL of candidate vaccines, containing 100 ng of either soluble or VLP-associated F-protein, were split equally over right and left quadriceps and administered to the mice. Two weeks after each immunization, blood was collected by tail vein bleed without anesthetics for serological assays.

C57Bl/6JOlaHsd mouse studies were performed by the team at IrsiCaixa, Badalona, Spain at the Centre for Comparative Medicine and Bioimage (CMCiB) under the approval of the Committee on the Ethics of Animal Experimentation of the Germans Trias i Pujol Research Institute (IGTP) and the authorization of Generalitat de Catalunya (codes: 9525). All procedures were in accordance with the 3R principle and prioritize animal welfare. 4 male and 4 female 6–8 weeks old C57Bl/6JOlaHsd mice (Envigo) were immunized twice with 4-weeks interval in the hock of one hindlimb with a maximum volume of 50 µl of vaccine containing 100 ng or 300 ng of either soluble or VLP-associated F-protein diluted in PBS and mixed with Adju-Phos (Invivogen, San Diego, USA) adjuvant at a 1:1 vol ratio. Housing conditions were 22+/−2 °C, 30–70 % humidity, 12 h dark/light cycle, and food and water *ad libitum*. 2 weeks after each immunization, a small blood sample was obtained from the facial vein under anesthesia (4–5 % isoflurane).

4.17. Immunogenicity analysis

Serum was recovered from whole blood by coagulation and centrifugation, and then were heat-inactivated at 56 °C for 30 min. Antibody binding titers against pre-fusion and post-fusion RSV-F and hMPV-F proteins were evaluated using ELISA. RSV pre-fusion F (DS-Cav1) [5], RSV post-fusion F [6] and hMPV F [32] coating antigens were produced as described previously. 384-well MaxiSorp treated plates (Thermo Scientific) were coated with 2 µg/mL of purified recombinant F protein and incubated overnight at 4 °C. Plates were then washed and blocked using 3 % milk in 1x PBS-T for 30 min at room temperature. Mouse sera were serially diluted in 10-point titration in 3 % milk in 1x PBS-T, transferred to the coated and blocked assay plates, and incubated at room temperature for 2 h. Plates were then washed 6 times with 1x PBS-T. After being washed, HRP conjugated goat anti-mouse antibody (Thermo Scientific) diluted at 1:10,000 in 3 % milk in 1x PBS-T was added to the plates, and the plates were incubated at room temperature for 1 h. Plates were washed again 6 times with 1x PBS-T and developed with West Pico PLUS Chemiluminescent Substrate (Thermo Scientific). After a 15-minute incubation at room temperature, luminescence was read on the EnVision 2104 microplate reader (PerkinElmer). An interpolated end point titer was calculated for each serum sample using the relative light unit (RLU) values and the following formula: interpolated endpoint titer = (starting dilution/series dilution factor) X (series dilution factor^t) where t = x − [(cut-off − L)/(H − L)]. The "cut-off" value was designated as 50,000. "H" = High well RLU value (the RLU value of the first titration point ABOVE 50,000), and "L" = Low well RLU value (the RLU of the first titration point BELOW 50,000). X = Low well number (the number in the titration series of "L", where the first dilution in the titration series was 1, and the highest serum dilution of the titration series was 10). Samples that did not cross the cut-off value were given a placeholder titer of "25", or one-half the initial starting serum dilution.

4.18. Neutralizing response analysis

Serum neutralization assays are conducted in 384-well plates and utilize an AlphaLISA-based assay readout which measures RSV or hMPV F protein present in cell lysates. Animal sera are heat inactivated and serially diluted in a 384-well plate. The sera are combined with virus and incubated for 1 h. Cells are added at a density of 5,000 cells per well, then further incubated for 72–96 h at 37 °C. After incubation, assay medium is removed, then cells and virus are lysed in AlphaLISA lysis buffer (PerkinElmer) for 60 min at room temperature. Diluted lysates from a set of four 384-well plates are combined into a 1536-well plate and then exposed to a suspension of AlphaLISA acceptor beads

(PerkinElmer) and biotinylated antibody for 1 h at room temperature. A suspension of streptavidin-coated donor beads (PerkinElmer) is next added to the plate and then further incubated at room temperature for 30 min, after which fluorescence is measured on an EnVision microplate reader (PerkinElmer). Four-parameter curve fitting (BioAssay analysis software) is used to calculate titers, from which the 50 % neutralizing titer (NT50) can be derived at the curve inflection point and reported as fold dilution. Separate assay setups used either RSV A Long or hMPV A Baylor at the virus addition step, and the differences between RSV and hMPV assays are described in Table 2.

4.19. Statistical analysis

All Figures were generated in GraphPad Prism 10.0.3. Statistical analyses were performed using R v4.1.1. Unpaired datasets were analyzed using a Kruskal-Wallis and Conover's post hoc test unless many results were undetected, in which case comparisons were performed with a Peto & Peto left-censored k sample test. Individual unpaired comparisons were performed with Mann-Whitney test and paired comparisons with Wilcoxon test.

CRediT authorship contribution statement

Benjamin Trinité: Writing – original draft, Methodology, Investigation, Formal analysis, Writing – review & editing. **Eberhard Durr:** Writing – review & editing, Writing – original draft, Investigation, Formal analysis. **Anna Pons-Grífols:** Writing – review & editing, Investigation. **Gregory O'Donnell:** Writing – review & editing, Writing – original draft, Investigation. **Carmen Aguilar-Gurrieri:** Writing – review & editing, Methodology, Investigation. **Silveria Rodriguez:** Writing – review & editing, Investigation. **Victor Urrea:** Writing – review & editing, Formal analysis. **Ferran Tarrés:** Writing – review & editing, Methodology. **Joel Mane:** Writing – review & editing, Investigation. **Raquel Ortiz:** Writing – review & editing, Investigation. **Carla Rovirosa:** Writing – review & editing, Investigation. **Jorge Carrillo:** Conceptualization, Writing – review & editing. **Bonaventura Clotet:** Writing – review & editing. **Lan Zhang:** Conceptualization, Supervision, Writing – original draft, Writing – review & editing. **Julià Blanco:** Conceptualization, Funding acquisition, Supervision, Writing – original draft, Writing – review & editing.

Declaration of competing interest

The authors declare the following financial interests/personal relationships which may be considered as potential competing interests: Julia Blanco reports financial support and equipment, drugs, or supplies were provided by Merck Sharp & Dohme Corp. Anna Pons-Grifols reports financial support was provided by Government of Catalonia Agency for Administration of University and Research Grants and European Social Fund. Julia Blanco reports a relationship with AlbaJuna Therapeutics SL that includes: board membership, employment, and equity or stocks. Jorge Carillo reports a relationship with AlbaJuna Therapeutics SL that includes: board membership, employment, and equity or stocks. Bonaventura Clotet reports a relationship with AlbaJuna Therapeutics SL that includes: board membership, employment, and equity or stocks. Eberhard Durr reports a relationship with Merck Sharp & Dohme Corp that includes: employment. Gregory O'Donnell reports a relationship with Merck Sharp & Dohme Corp that includes: employment. Silveria Rodriguez reports a relationship with Merck Sharp & Dohme Corp that includes: employment. Joel Mane reports a relationship with Merck Sharp & Dohme Corp that includes: employment. Lan Zhang reports a relationship with Merck Sharp & Dohme Corp that includes: employment. Eberhard Durr reports a relationship with Merck & Co Inc that includes: equity or stocks. Gregory O'Donnell reports a relationship with Merck & Co Inc that includes: equity or stocks. Silveria Rodriguez reports a relationship with Merck & Co Inc that includes: equity or stocks. Joel Mane reports a relationship with Merck & Co Inc that includes: equity or stocks. Lan Zhang reports a relationship with Merck & Co Inc that includes: equity or stocks. Bonaventura Clotet has patent #EP1638234.4 "Virus-like particles with high density coating for the production of neutralizing antibodies" licensed to Irsicaixa. Jorge Carrillo has patent #EP1638234.4 "Virus-like particles with high density coating for the production of neutralizing antibodies" licensed to Irsicaixa. Julia Blanco has patent #EP1638234.4 "Virus-like particles with high density coating for the production of neutralizing antibodies" licensed to Irsicaixa. If there are other authors, they declare that they have no known competing financial interests or personal relationships that could have appeared to influence the work reported in this paper.

Table 2
Comparison of serum neutralization assay conditions for RSV and hMPV.

Assay condition	RSV	hMPV
Virus concentration added	25 pfu/well	65 pfu/well
Host cell line	Hep2	Vero CCL-81
Incubation time at 37 °C, 5 % CO_2, 80 % RH	72 hrs	96 hrs
$CaCl_2$ in assay medium	None	0.03 %
Cell/virus lysate dilution factor	1:50	1:10
Acceptor bead antibody	1D2 M2D2 (Merck & Co., Inc., Rahway, NJ, USA)	MCA4674 (Bio-Rad)
Biotinylated antibody	10-R25C (Fitzgerald)	M2D2 (Merck & Co., Inc., Rahway, NJ, USA)

Data availability

Data will be made available on request.

Acknowledgements

This study was funded by Merck & Co., Inc. Kenilworth, NJ, USA. We would like to thank Jennifer Galli, Scott Cosmi and Gwenny Go for expression and purification of the recombinant VCR4 and hMPV proteins that were used in this study, Zhifeng Chen for providing the antibodies used for VLP characterization, and Joseph Osinubi for technical assistance in the virus neutralization assays. Special thanks to Andrew Bett, Kalpit Vora, and Ming-Tang Chen for their expert advice and helpful comments for the study. A.P-G. was supported by a predoctoral grant from Generalitat de Catalunya, Spain and Fons Social Europeu (2022 FI_B 00698).

Author contributions

BT generated the VLPs, performed *in vitro* and *in vivo* experiments, and drafted the manuscript. **ED** performed the Mass Spec analyses and drafted the manuscript. **APG** performed *in vivo* experiments. **GD** performed serum ELISA assays and drafted the manuscript. **CA** performed the cryo-EM analyses and contributed to the optimization of the VLP platform. **SR** performed serum neutralization assays. **VU** performed statistical analyses. **FT** contributed to the optimization of the VLP platform. **JM** performed *in vivo* BALB/c mouse study. **RO** performed western blot and ELISA experiments. **CR** performed molecular cloning and western blot experiments. **JC** designed the study. **BC** designed the study. **LZ** designed the study and drafted the manuscript**. JB** designed the study and drafted the manuscript. All authors corrected the manuscript and approved the submitted version.

Appendix A. Supplementary material

Supplementary data to this article can be found online at https://doi.org/10.1016/j.vaccine.2024.04.048.

References

[1] Wang X, Li Y, Deloria-Knoll M, et al. Global burden of acute lower respiratory infection associated with human metapneumovirus in children under 5 years in 2018: a systematic review and modelling study. Lancet Glob Heal 2021;9(1): e33–43. https://doi.org/10.1016/S2214-109X(20)30393-4.

[2] Maggi S, Veronese N, Burgio M, et al. Rate of hospitalizations and mortality of respiratory syncytial virus infection compared to influenza in older people: a systematic review and meta-analysis. Vaccines 2022;10(12):2092. https://doi.org/10.3390/VACCINES10122092/S1.

[3] Young M, Smitherman L. Socioeconomic impact of RSV hospitalization. Infect Dis Ther 2021;10(1):35–45. https://doi.org/10.1007/S40121-020-00390-7/FIGURES/2.

[4] McLellan JS, Yang Y, Graham BS, Kwong PD. Structure of respiratory syncytial virus fusion glycoprotein in the postfusion conformation reveals preservation of neutralizing epitopes. J Virol 2011;85(15):7788–96. https://doi.org/10.1128/JVI.00555-11.

[5] McLellan JS, Chen M, Leung S, et al. Structure of RSV fusion glycoprotein trimer bound to a prefusion-specific neutralizing antibody. Science 2013;340(6136): 1113–7. https://doi.org/10.1126/science.1234914.

[6] Swanson KA, Settembre EC, Shaw CA, et al. Structural basis for immunization with postfusion respiratory syncytial virus fusion F glycoprotein (RSV F) to elicit high neutralizing antibody titers. Proc Natl Acad Sci 2011;108(23):9619–24. https://doi.org/10.1073/pnas.1106536108.

[7] Johnson S, Oliver C, Prince GA, et al. Development of a humanized monoclonal antibody (MEDI-493) with potent in vitro and in vivo activity against respiratory syncytial virus. J Infect Dis 1997;176(5):1215–24. https://doi.org/10.1086/514115.

[8] Palivizumab, a humanized respiratory syncytial virus monoclonal antibody, reduces hospitalization from respiratory syncytial virus infection in high-risk infants. Pediatrics 1998;102(3):531–7. Accessed April 3, 2023. http://www.ncbi.nlm.nih.gov/pubmed/9724660.

[9] Glezen WP. Risk of primary infection and reinfection with respiratory syncytial virus. Arch Pediatr Adolesc Med 1986;140(6):543. https://doi.org/10.1001/archpedi.1986.02140200053026.

[10] Falsey AR, Walsh EE. Relationship of serum antibody to risk of respiratory syncytial virus infection in elderly adults. J Infect Dis 1998;177(2):463–6. https://doi.org/10.1086/517376.

[11] Piedra P. Correlates of immunity to respiratory syncytial virus (RSV) associated-hospitalization: establishment of minimum protective threshold levels of serum neutralizing antibodies. Vaccine 2003;21(24):3479–82. https://doi.org/10.1016/S0264-410X(03)00355-4.

[12] Hsieh CL, Rush SA, Palomo C, et al. Structure-based design of a fusion glycoprotein vaccine for respiratory syncytial virus. Science 2013;342(6158):592–8. https://doi.org/10.1126/science.1243283.

[13] Ingale J, Stano A, Guenaga J, et al. High-density array of well-ordered HIV-1 spikes on synthetic liposomal nanoparticles efficiently activate B cells. Cell Rep 2016;15 (9):1986–99. https://doi.org/10.1016/j.celrep.2016.04.078.

[14] Steichen JM, Kulp DW, Tokatlian T, et al. HIV vaccine design to target germline precursors of glycan-dependent broadly neutralizing antibodies. Immunity 2016; 45(3):483–96. https://doi.org/10.1016/j.immuni.2016.08.016.

[15] Jardine J, Julien J-P, Menis S, et al. Rational HIV immunogen design to target specific germline B cell receptors. Science 2013;340(6133):711–6. https://doi.org/10.1126/science.1234150.

[16] Blanco JCG, Fernando LR, Zhang W, et al. Alternative virus-like particle-associated prefusion F proteins as maternal vaccines for respiratory syncytial virus. Dutch RE, ed. J Virol. 2019;93(23). doi:10.1128/JVI.00914-19.

[17] Cox RG, Erickson JJ, Hastings AK, et al. Human metapneumovirus virus-like particles induce protective B and T cell responses in a mouse model. Lyles DS, ed. J Virol. 2014;88(11):6368–79. doi:10.1128/JVI.00332-14.

[18] Ha B, Yang JE, Chen X, Jadhao SJ, Wright ER, Anderson LJ. Two RSV platforms for G, F, or G+F proteins VLPs. Viruses 2020;12(9):906. https://doi.org/10.3390/v12090906.

[19] Luo J, Qin H, Lei L, Lou W, Li R, Pan Z. Virus-like particles containing a prefusion-stabilized F protein induce a balanced immune response and confer protection against respiratory syncytial virus infection in mice. Front Immunol 2022:13. https://doi.org/10.3389/fimmu.2022.1054005.

[20] McGinnes Cullen L, Luo B, Wen Z, Zhang L, Durr E, Morrison TG. The respiratory syncytial virus (RSV) G protein enhances the immune responses to the RSV F protein in an enveloped virus-like particle vaccine candidate. Dutch RE, ed. J Virol 2023;97(1). doi:10.1128/jvi.01900-22.

[21] McGinnes Cullen L, Schmidt MR, Kenward SA, Woodland RT, Morrison TG. Murine immune responses to virus-like particle-associated pre- and postfusion forms of the respiratory syncytial virus F protein. Lyles DS, ed. J Virol 2015;89(13):6835–47. doi:10.1128/JVI.00384-15.

[22] Marcandalli J, Fiala B, Ols S, et al. Induction of potent neutralizing antibody responses by a designed protein nanoparticle vaccine for respiratory syncytial virus. Cell 2019;176(6):1420–1431.e17. https://doi.org/10.1016/j.cell.2019.01.046.

[23] Nooraei S, Bahrulolum H, Hoseini ZS, et al. Virus-like particles: preparation, immunogenicity and their roles as nanovaccines and drug nanocarriers. J Nanobiotechnology 2021;19(1):59. https://doi.org/10.1186/s12951-021-00806-7.

[24] Tarrés-Freixas F, Aguilar-Gurrieri C, Rodríguez de la Concepción ML, et al. An engineered HIV-1 Gag-based VLP displaying high antigen density induces strong antibody-dependent functional immune responses. npj Vaccines 2023;8(1):51. https://doi.org/10.1038/s41541-023-00648-4.

[25] Ortiz R, Barajas A, Pons-Grífols A, et al. Exploring FeLV-gag-based VLPs as a new vaccine platform—analysis of production and immunogenicity. Int J Mol Sci 2023; 24(10):9025. https://doi.org/10.3390/ijms24109025.

[26] Joyce MG, Zhang B, Ou L, et al. Iterative structure-based improvement of a fusion-glycoprotein vaccine against RSV. Nat Struct Mol Biol 2016;23(9):811–20. https://doi.org/10.1038/NSMB.3267.

[27] Arumugham RG, Seid RC, Doyle S, Hildreth SW, Paradiso PR. Fatty acid acylation of the fusion glycoprotein of human respiratory syncytial virus. J Biol Chem 1989; 264(18):10339–42. http://www.ncbi.nlm.nih.gov/pubmed/2732224.

[28] Branigan PJ, Day ND, Liu C, et al. The cytoplasmic domain of the F protein of Human respiratory syncytial virus is not required for cell fusion. J Gen Virol 2006; 87(2):395–8. https://doi.org/10.1099/vir.0.81481-0.

[29] Flynn JA, Durr E, Swoyer R, et al. Stability characterization of a vaccine antigen based on the respiratory syncytial virus fusion glycoprotein. Mantis NJ, ed. PLoS One 2016;11(10):e0164789. doi:10.1371/journal.pone.0164789.

[30] Kwakkenbos MJ, Diehl SA, Yasuda E, et al. Generation of stable monoclonal antibody–producing B cell receptor–positive human memory B cells by genetic programming. Nat Med 2010;16(1):123–8. https://doi.org/10.1038/nm.2071.

[31] Xiao X, Tang A, Cox KS, et al. Characterization of potent RSV neutralizing antibodies isolated from human memory B cells and identification of diverse RSV/hMPV cross-neutralizing epitopes. MAbs 2019;11(8):1415–27. https://doi.org/10.1080/19420862.2019.1654304.

[32] Xiao X, Fridman A, Zhang L, et al. Profiling of hMPV F-specific antibodies isolated from human memory B cells. Nat Commun 2022;13(1):2546. https://doi.org/10.1038/s41467-022-30205-x.

[33] Beeler JA, van Wyke CK. Neutralization epitopes of the F glycoprotein of respiratory syncytial virus: effect of mutation upon fusion function. J Virol 1989;63 (7):2941–50. https://doi.org/10.1128/jvi.63.7.2941-2950.1989.

[34] Crank MC, Ruckwardt TJ, Chen M, et al. A proof of concept for structure-based vaccine design targeting RSV in humans. Science 2019;365(6452):505–9. https://doi.org/10.1126/science.aav9033.

[35] Kee GS, Jin J, Balasundaram B, Bracewell DG, Pujar NS, Titchener-Hooker NJ. Exploiting the intracellular compartmentalization characteristics of the S. cerevisiae host cell for enhancing primary purification of lipid-envelope virus-like particles. Biotech. Prog. Published online 2009. https://doi.org/10.1002/btpr.307.

[36] Kee GS, Pujar NS, Titchener-Hooker NJ. Study of detergent-mediated liberation of hepatitis B virus-like particles from S. cerevisiae homogenate: identifying a framework for the design of future-generation lipoprotein vaccine processes. Biotechnol Prog 2008;24(3):623–31. https://doi.org/10.1021/bp070472i.

[37] Malyala P, Singh M. Endotoxin limits in formulations for preclinical research. J Pharm Sci 2008;97(6):2041–4. https://doi.org/10.1002/jps.21152.

[38] Cimica V, Boigard H, Bhatia B, et al. Novel respiratory syncytial virus-like particle vaccine composed of the postfusion and prefusion conformations of the F glycoprotein. Pasetti MF, ed. Clin Vaccine Immunol 2016;23(6):451–9. doi: 10.1128/CVI.00720-15.

[39] Cullen L, Schmidt M, Torres G, Capoferri A, Morrison T. Comparison of immune responses to different versions of VLP associated stabilized RSV pre-fusion F protein. Vaccines 2019;7(1):21. https://doi.org/10.3390/vaccines7010021.

[40] Hsieh CS, Macatonia SE, O'Garra A, Murphy KM. T cell genetic background determines default T helper phenotype development in vitro. J Exp Med 1995;181 (2):713–21. https://doi.org/10.1084/jem.181.2.713.

[41] Stewart D, Fulton WB, Wilson C, et al. Genetic contribution to the septic response in a mouse model. Shock 2002;18(4):342–7. https://doi.org/10.1097/00024382-200210000-00009.

[42] Wen X, Krause JC, Leser GP, et al. Structure of the human metapneumovirus fusion protein with neutralizing antibody identifies a pneumovirus antigenic site. Nat Struct Mol Biol 2012;19(4):461–3. https://doi.org/10.1038/nsmb.2250.

[43] Wiśniewski JR. Filter-aided sample preparation: the versatile and efficient method for proteomic analysis. Methods Enzymol 2017;585:15–27. https://doi.org/10.1016/BS.MIE.2016.09.013.